Inducing dispersion curves with negative group velocity in inertially amplified phononic crystals through the application of an external state of prestress

M. Miniaci, M. Mazzotti, A. Amendola, F. Fraternali

Available online at www.easdprocedia.org
EASD Procedia EURODYN (2020) 612-620

EASD Procedia

EURODYN 2020
XI International Conference on Structural Dynamics
M. Papadrakakis, M. Fragiadakis, C. Papadimitriou (eds.)
Athens, Greece, 23–26 November 2020

INDUCING DISPERSION CURVES WITH NEGATIVE GROUP VELOCITY IN INERTIALLY AMPLIFIED PHONONIC CRYSTALS THROUGH THE APPLICATION OF AN EXTERNAL STATE OF PRESTRESS

M. Miniaci[1], M. Mazzotti[2], A. Amendola[3] and F. Fraternali [3]

[1]CNRS, Centrale Lille, ISEN, Univ. Lille, Univ. Valenciennes, UMR 8520 - IEMN
F-59000 Lille, France
e-mail: marco.miniaci@univ-lille.fr, marco.miniaci@gmail.com

[2] Department of Mechanical Engineering, CU Boulder
Boulder, CO 80309, USA e-mail: matteo.mazzotti@gmail.com

[3] Department of Civil Engineering, University of Salerno
Salerno, Italy
e-mail:{adaamendola1, f.fraternali}@unisa.it

Keywords: Phononic Crystals and Metamaterials, Prestress / Prestrain, Band Diagram Tunability, Inertial Amplification Mechanism.

Abstract. *In this paper, we report about the effect of the application of a state of prestress on the band structure of a periodic phononic crystal characterized by an inertial amplification mechanism. Through a numerical example, we show the possibility of inducing negative group velocity in an isolated branch of the dispersion diagram.*
A 2-step Updated Lagrangian scheme is adopted to calculate the dispersion diagram of the structure. The proposed method include (i) the static geometrically nonlinear analysis of a representative unit cell undergoing the action of an applied external load and (ii) the Bloch-Floquet decomposition applied to the linearized equations of the acousto-elasticity for the unit cell in the deformed configuration. The dispersion analysis is performed in terms of small amplitude motions superimposed on a deformed state, once the desired load has been applied.

ISSN:2311-9020
Peer-review under responsibility of the Organizing Committee of EURODYN 2020.
doi: 10.47964/1120.9048.21611

1 Introduction

Controlling the propagation of elastic waves in solids has always attracted the interest of physicists and engineers. Considerable progress has been made in this area thanks to the introduction in the last decades of the so called *phononic crystals* and *elastic metamaterials*, i.e., artificial periodic structures with variations in density / stiffness / geometry, exhibiting unconventional dynamic properties, such as for instance frequency regions where the propagation of waves is inhibited, referred to as phononic bandgaps, or negative group velocity of their branches [1], allowing for negative refraction [2].
Since their introduction, a plethora of innovative applications relying on frequency filtering [3], topological protection [4, 5] and wave splitting [6] have been proposed in the most disparate fields ranging from the infrasonic to the ultrasonic frequency regime [7–11].
However, one of the main limitations of these structures is represented by the fact that once designed, their unusual dynamic properties are fixed in terms of operational frequency. For example, a metamaterial designed and manufactured to attain specific unconventional properties in a certain frequency range (for instance attenuating the propagation of elastic waves or exhibiting negative group velocity) cannot be modified to operate in a different frequency range. This implies poor versatility and adaptability to external variations, often essential for various practical applications.
In this context, periodic systems with adaptive elastic properties have been proposed tuning the dispersion diagrams through the piezoelectric effect [12, 13], inducing temperature variation [14], or exployting magneto- and light-based approaches [15, 17], as well as applying external mechanical loads [18–22].
The majority of the aforementioned investigations focused their attention on the bandgap shift / widening / reduction, whereas here, we report about the possibility of inducing negative group velocity in an isolated branch of the dispersion diagram of an inertially amplified phononic crystals. This is achieved through the application of an external state of prestress. A phononic crystal exhibiting inertial amplification mechanism has been chosen because it has been shown that the large inertial forces generated by amplifying the motion of a mass increases the inertia of the overall system and lowers its resonance frequency, allowing thus for sub-wavelength phenomena, while keeping the structure lightweight [25, 26]. As a consequence of this, the inertial amplification allows for a more remarkable curve shifts, if compared to the cases of Bragg scattering [21, 22] and / or ordinary local resonant metamaterials.
We consider the static deformation induced by the prestress to be in the linear elastic regime so to have a complete reversibility of the phenomena (tunability). The analysis is performed in terms of small amplitude motions superimposed on a deformed state once the desired load has been applied.
The paper is organized as follows: in section 2, the calculation method (referred to as a *2-step Updated Lagrangian scheme*) is briefly recalled. Both the static geometrically nonlinear analysis of a representative unit cell undergoing the action of an applied external load and the Bloch-Floquet decomposition applied to the linearized equations of the acousto-elasticity for the unit cell in the deformed configuration, are recalled. Section 3 provides a numerical example showing the concrete possibility of altering the dispersion band diagram through the application of an external state of prestress in a periodic structure exhibiting inertial amplification mechanism. Finally, section 4 synthesizes the principal results and provides future perspectives.

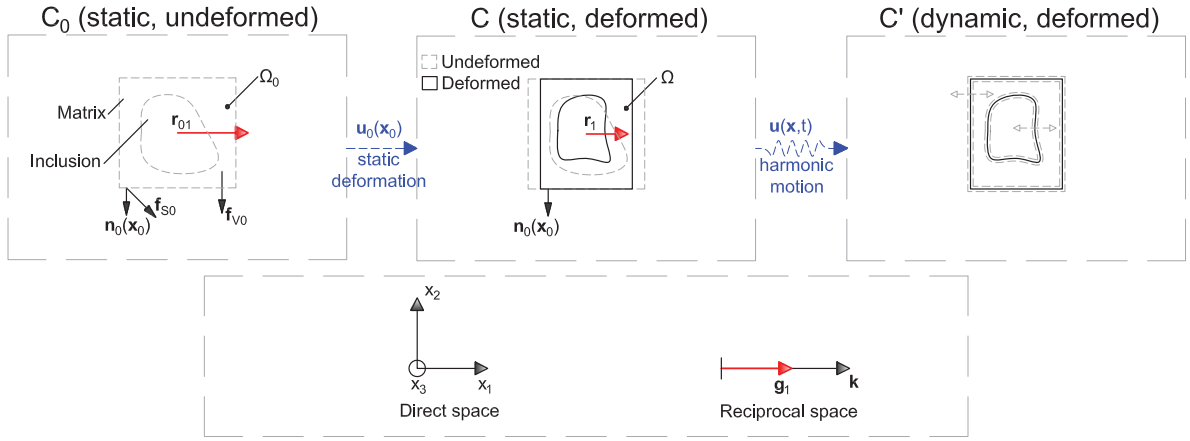

Figure 1: On the top panel, the undeformed configuration C_0, i.e. the initial unit cell (delimited by dashed lines) used to calculate the displacement and stress fields introduced by the external mechanical load (left panel), the static deformed configuration C, resulting from the application of the external mechanical load (middle panel) and the dynamic configuration C' undergoing a harmonic motion (right panel) are reported, respectively. In the bottom panel, the reference systems in the direct and reciprocal spaces are reported as well, for the sake of completeness.

2 Numerical formulation: a brief recall of the 2-step Updated Lagrangian scheme

We here recall the main steps for the band diagram calculation adopting a Bloch-Floquet finite element method which takes into account the effect of the prestress in a formulation called 2-step Updated Lagrangian scheme. Refer to [21, 22] for the full description of the approach. Synthesizing, the numerical procedure includes two principal computational steps:

1) a nonlinear static analysis involving large strains and displacements;

2) a *small-on-large* dynamic analysis, in which small vibrations are superimposed to the statically deformed unit cell.

2.1 Static analysis

Let's consider the unit cell Ω_0 represented on the top left panel of Fig. 1 by the gray dashed line. The unit cell is identified by the position vector $\mathbf{x}$ and represented by the lattice vector $\mathbf{r}_0 = \{r_{01}, 0\}^{\mathrm{T}}$ (periodicity only in the x direction is considered) and its reciprocal vector $\mathbf{g}_0 = \{g_{01}, 0\}^{\mathrm{T}} = \{r_{01}/2\pi, 0\}^{\mathrm{T}}$. If the unit cell is subjected to the application of a static volume load $\mathbf{f}_{V0}$, or surface load $\mathbf{f}_{S0}$, it undergoes a displacement $\mathbf{u}_0$, which causes a change of configuration from the undeformed state C_0 to the static deformed state C.
It is possible to write the relation between $\mathbf{r}_0$ and $\mathbf{r}$ as $\mathbf{r} = \mathbf{F}_L\mathbf{r}_0$, where $\mathbf{F}_L$ defines the affine component of the deformation gradient. Making use of the variational statement, it is possible to derive the equilibrium equations with respect to the undeformed configuration C_0:

$$\int_{\Omega} \left(\mathbf{S}(\mathbf{x}) : \delta\mathbf{E}(\mathbf{x}) - \mathbf{f}_{V0} \cdot \delta\mathbf{u}_0\right) da = \int_{\partial\Omega} \mathbf{f}_{s0} \cdot \delta\mathbf{u}_0 ds, \tag{1}$$

subjected to the Dirichlet boundary conditions:

$$\mathbf{u}_0(\mathbf{x} + \mathbf{r}_0) = \mathbf{u}_0(\mathbf{x}). \tag{2}$$

Assuming a hyperelastic material according to the Murnaghans model [27–29] and specifying the density of the unit cell as ρ_0, the elastic energy density can be defined as:

$$\psi = \frac{1}{2}\left(\lambda + 2\mu\right) I_1^2(\mathbf{E}) - 2\mu I_2(\mathbf{E}) + \frac{1}{3}\left(l + 2m\right) I_1^3(\mathbf{E}) - 2m I_1(\mathbf{E}) I_2(\mathbf{E}) + n I_3(\mathbf{E}), \tag{3}$$

in which λ and μ denote the first and second Lamé parameters, respectively, (l, m, n) the third order Murnaghan parameters, and $I_1(\mathbf{E})$, $I_2(\mathbf{E})$ and $I_3(\mathbf{E})$ the first, second and third invariants of the Green-Lagrange strain tensor, respectively.
The application of a standard Galerkin approach to Eq. (1) leads to the generalized system of equations:

$$\left[\mathbf{\Gamma}_0^{\mathrm{T}} \mathbf{K}(\mathbf{Q}_0) \mathbf{\Gamma}_0\right] \mathbf{Q}_0(\mathbf{X}) = \mathbf{P}_0(\mathbf{X}), \tag{4}$$

where $\mathbf{K}(\mathbf{Q}_0)$ is the static stiffness matrix, $\mathbf{P}_0$ the global vector of nodal forces, $\mathbf{Q}_0$ the global vector of independent nodal displacements and $\mathbf{\Gamma}_0$ the mapping operator resulting from Eq. (2) and realizing the condition $\mathbf{U}_0 = \mathbf{\Gamma}_0 \mathbf{Q}_0$. This will allow us to update the reference configuration from C_0 to C, which will be used, once properly re-meshed, as the basis unit cell for the dispersion curve calculation.

2.2 Floquet-Bloch Analysis

Under the assumption of *small-on-large analysis approach* [28, 30–32], the small harmonic perturbation $\mathbf{u}(\mathbf{x})$ can be expressed as [33]:

$$\mathbf{u}(\mathbf{x}) = \tilde{\mathbf{u}}(\mathbf{x}) \exp(\mathrm{i}kx) \exp(-\mathrm{i}\omega t), \tag{5}$$

in which the Ω-periodic displacement amplitude is taken into account (t denotes the time, ω the angular frequency, and $k \in \Lambda$ the Bloch wavenumber, being Λ the reciprocal unit cell defined in C by the reciprocal lattice vector.
The solution of the elastodynamic problem for free vibrations of the unit cell in C subjected to an initial stress $\boldsymbol{\sigma}_0$ and subjected to the Dirichlet boundary condition proceeds by first generating a new mesh for the deformed geometry of the unit cell in C and then applying a Galerkin approach [34]. The band diagrams of the phononic structure can be computed from the eigenvalue problem (the mathematical expressions of the mapping operator implementing the Dirichlet boundary condition, $\mathbf{K}_3$, $\mathbf{K}_2$, $\mathbf{K}_1$ and $\mathbf{M}$ are not reported in the present paper for the sake of brevity and can be found in Refs. [21, 22]):

$$\left\{\mathbf{\Gamma}^{\mathrm{T}} \left[k^2 \mathbf{K}_3 + \mathrm{i}k \left(\mathbf{K}_2 - \mathbf{K}_2^{\mathrm{T}}\right) + \mathbf{K}_1 - \omega^2 \mathbf{M}\right] \mathbf{\Gamma}\right\} \tilde{\mathbf{Q}}(\omega) = \mathbf{0}. \tag{6}$$

3 Numerical results

In this section, the potential of an applied external mechanical load to alter the dispersion diagram of a periodic structure characterized by an inertial amplification mechanism is shown. Specifically, the switching from positive to negative group velocity of an isolated dispersion curve is reported.
To this aim, the band diagram is calculated for the unit cell reported in Fig. 2A (proposed for the first time by Acar and Yilmaz [26]) through the numerical procedure recalled in section 2. The structure is supposed to be in epoxy with the following material parameters: $\rho = 1540$ kg/m^3, $\lambda = 2.59$ GPa, $\mu = 1.34$ GPa, $l = -18.94$, GPa, $m = -13.36$ GPa and $n = -9.81$ GPa. The geometrical dimensions can be derived from Fig. 2A knowing that $t_2 = 0.4$ mm has been assumed.

Once the deformation induced in the unit cell by an initial state of stress / strain applied to the structure has been calculated according to the steps reported in section 2.1, the band structures are computed considering the unit cell to infinitely duplicate in a periodic linear array, and assuming the epoxy in its linear elastic regime and under the hypothesis of small displacements (see section 2.2). Both a compression and a traction condition of load are considered by applying a displacement $\mathbf{u}_0(\mathbf{x}_0) \cdot \mathbf{n}_0(\mathbf{x}_0)$ normal to the external vertical faces of the unit cell (highlighted in blue in Fig. 2A).
Figure 2B reports the plots of the the reduced wavenumber k^* along the $\Gamma - X$ irreducible path as a function of the frequency ([$0 - 900$ Hz range]) for $+130$ μm (left panel), 0 μm (central panel) and -360 μm (right panel) assigned prestrains. We focus our attention on the dispersion branch highlighted in purple, which, in contrast to the other branches reported in gray, besides a general shift, undergoes a group velocity inversion for some values of the reduced wavenumber k^*. Specifically, if inducing a pre-solicitation state of traction, the inflexion point is achieved around $k^* \simeq 0.5\pi/a$, whereas, when inducing a state of pre-compression, the transition occurs for $k^* \simeq 0.65\pi/a$ (black arrows in Fig. 2B). To gain further insight on this phenomenon, the corresponding mode shape evaluated at the high symmetry points Γ and X are inspected and reported in Fig. 2C. From the comparison it emerges that while the vibration pattern is practically the same for low values of k^* (the 3 mode shapes denoted by the star symbol deform comparably), as the k^* increases, the deformation induced by the states of prestress alter the overall deformation mechanism with respect to the non-prestressed case (compare the 3 modes denoted by the circular dot). This change in the deformation mode happens only for this branch. As a consequence, for the other branches reported in gray in the diagram the effect of the prestress is to solely shift their frequencies. This allows us to infer that the prestress is differently felt from the deformation modes of the phononic crystal.
Finally, it is worth noticing that in the first pre-solicitation case (traction), a region in which solely the negative group velocity part of the dispersion branch can be isolated in frequency (see the orange dashed line and the orange arrow in Fig. 2B) from 525 to 550 Hz.
These results suggest that a deformation of the unit cell geometry induced by a compressive / tensile prestress state, already in the elastic regime, can lead to significant changes in the dynamic behaviour of a periodic structure, especially if the structure is dominated by an inertial amplification mechanism.

4 Concluding remarks

In this paper, we have reported about the effect of the application of a state of prestress on the band structure of a periodic phononic crystal characterized by an inertial amplification mechanism. Specifically, through a numerical example, we have shown the possibility of inducing negative group velocity in an isolated branch of the dispersion diagram.
The dispersion curves are calculated through a *2-step Updated Lagrangian scheme* within the which both the static geometrically nonlinear analysis of a representative unit cell undergoing the action of an applied external load and the Bloch-Floquet decomposition applied to the linearized equations of the acousto-elasticity for the unit cell in the deformed configuration, are implemented. The dispersion analysis is performed in terms of small amplitude motions superimposed on a deformed state, once the desired load has been applied. It is worth mentioning that we have considered the static deformation induced by the prestress to be in the linear elastic regime, so to guarantee a complete reversibility of the phenomena, once the load removed.
This study may represent a practical solution for reducing one of the limitations of phononic crystals / metamaterials, represented by the fact that once designed, their unusual dynamic prop-

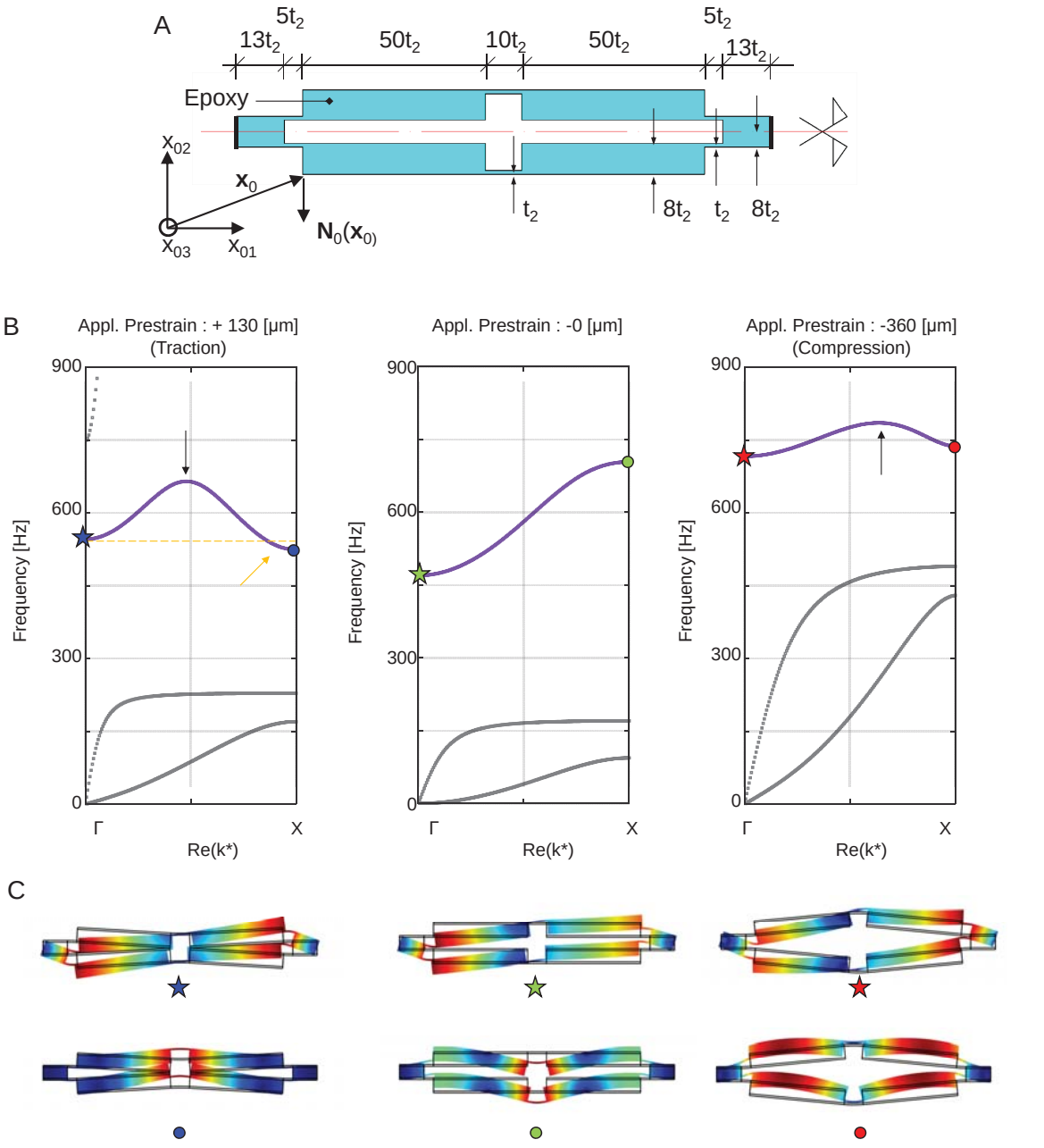

Figure 2: (A) Schematic representation of the considered unit cell along with its position $\mathbf{x}_0$ with respect to the original reference systems x_{0i}, with i = 1,2,3. (B) Plots of the the reduced wavenumber k^* along the $\Gamma - X$ irreducible path as a function of the frequency for $+130$ μm (left), 0 μm (centre) and -360 μm (right) prestrain conditions. (C) Mode shapes at the edges of the $\Gamma - X$ irreducible path.

erties are fixed in terms of operational frequency.
Future research may include the application of additional internal state of prestress (for instance exploiting the tensegrity paradigm) to foster the application of phononic crystals and metamaterials in engineering problems such as waveguiding / filtering of elastic waves, impact protection, and the design of tunable acoustic lenses.

Acknowledgements

FF acknowledges financial support from the Italian Ministry of Education, University and Research (MIUR) under the P.R.I.N. 2017 National Grant‘ Multiscale Innovative Materials and Structures’ (Project Code 2017J4EAYB).

REFERENCES

[1] Deymier P. A., (eds) 2013. Acoustic Metamaterials and Phononic Crystals, Springer Series in Solid-State Sciences (Springer Berlin Heidelberg).

[2] Morvan, B., Tinel, A., Hladky-Hennion, A.-C., Vasseur, J.O., Dubus, B., 2010. Experimental demonstration of the negative refraction of a transverse elastic wave in a two-dimensional solid phononic crystal Appl. Phys. Lett. 96, 101905.

[3] Hussein, M.I., Leamy, M.J., Ruzzene, M., 2014. Dynamics of phononic materials and structures: Historical origins, recent progress, and future outlook, Applied Mechanics Reviews 66, 040802.

[4] Mousavi, H., Khanikaev, A.B., Wang, Z., 2015. Topologically protected elastic waves in phononic metamaterials, Nat. Commun. 6, 8682.

[5] Miniaci, M., Pal, R.K., Morvan, B., Ruzzene, M., 2018. Experimental observation of topologically protected helical edge modes in patterned elastic plates, Phys. Rev. X 8, 031074.

[6] Miniaci, M., Pal, R.K., Manna, R., Ruzzene, M., 2019. Valley-based splitting of topologically protected helical waves in elastic plates, Phys. Rev. B 100, 024304.

[7] Miniaci, M., Gliozzi, A.S., Morvan, B., Krushynska, A.K., Bosia, F., Scalerandi, M., Pugno, N.M., 2017. Proof of concept for an ultrasensitive technique to detect and localize sources of elastic nonlinearity using phononic crystals, Phys. Rev. Lett. 118, 214301.

[8] Brûlé, S., Javelaud, E.H., Enoch, S., Guenneau, S., 2014. Experiments on seismic metamaterials: Molding surface waves, Phys. Rev. Lett. 112, 133901.

[9] Miniaci, M., Krushynska, A., Bosia, F., Pugno, N.M., 2016. Large scale mechanical metamaterials as seismic shields, New Journal of Physics 18, 083041.

[10] Fraternali, F., Amendola, A., Benzoni, G., 2018. Innovative seismic isolation devices based on lattice materials: A review, Ing. Sismica 4, 93–113.

[11] Misseroni, D., Colquitt, D.J., Movchan, A.B., Movchan, N.V., Jones, I.S., 2016. Cymatics for the cloaking of flexural vibrations in a structured plate, Scientific Reports 6, 23929.

[12] Bergamini, A., Delpero, T., De Simoni, L., Di Lillo, L., Ruzzene, M., Ermanni, P., 2014. Phononic crystal with adaptive connectivity, Advanced Materials 26, 1343–1347.

[13] Kherraz, N., Haumesser, L., Levassort, F., Benard, P., Morvan, B., 2016. Controlling Bragg gaps induced by electric boundary conditions in phononic piezoelectric plates, Applied Physics Letters 108, 093503.

[14] Jim, K.L., Leung, C.W., Lau, S.T., Choy, S.H., Chan, H.L.W., 2009. Thermal tuning of phononic bandstructure in ferroelectric ceramic/epoxy phononic crystal, Applied Physics Letters 94, 193501.

[15] Robillard, J.-F., Bou Matar, O., Vasseur, J.O., Deymier, P.A., Stippinger, M., Hladky-Hennion, A.-C., Pennec, Y., Djafari-Rouhani, B., 2009. Tunable magnetoelastic phononic crystals, Applied Physics Letters 95, 124104.

[16] Bou Matar, O., Robillard, J.-F., Vasseur, J.O., Hladky-Hennion, A.-C., Deymier, P.A., Pernod, P., Preobrazhensky, P., 2012. Band gap tunability of magneto-elastic phononic crystal, Journal of Applied Physics 111, 054901.

[17] Gliozzi, A.S., Miniaci, M., Chiappone, A., Bergamini, A., Morin, B., Descrovi, E., 2020. Photo-responsive tunable elastic metamaterials, Nat. Commun. (in press).

[18] Bordiga, G., Cabras, L., Piccolroaz, A., Bigoni, D., 2019. Prestress tuning of negative refraction and wave channeling from flexural sources, Applied Physics Letters 114, 041901.

[19] Bigoni, D., Gei, M., Movchan, A.B., 2008. Dynamics of a prestressed stiff layer on an elastic half space: filtering and band gap characteristics of periodic structural models derived from long-wave asymptotics, Journal of the Mechanics and Physics of Solids 56, 2494–2520.

[20] Gei, M., 2010. Wave propagation in quasi-periodic structures: stop/pass band distribution and prestress effects, International Journal of Solids and Structures 47, 3067–3075.

[21] Mazzotti, M., Bartoli, I., Miniaci, M., 2019. Modeling Bloch waves in prestressed phononic crystal plates, Frontiers in Materials 6, 74.

[22] Miniaci, M., Mazzotti, M., Amendola, A., Fraternali, F., 2020. Effect of prestress on phononic band gaps induced by inertial amplification, (in revision)

[23] Amendola, A. Carpentieri, G., de Oliveira, M., Skelton, R., Fraternali, F., 2014. Experimental investigation of the softening / stiffening response of tensegrity prisms under compressive loading, Composite Structures 117, 234–243.

[24] Slesarenko, V., Galich, P.I., Li, J., Fang, N.X., Rudykh, S., 2018. Foreshadowing elastic instabilities by negative group velocity in soft composites, Applied Physics Letters 113, 031901.

[25] Yilmaz, C., Hulbert, G.M., Kikuchi, N., 2007. Phononic band gaps induced by inertial amplification in periodic media, Physical Review B - Condensed Matter and Materials Physics 76.

[26] Acar, G., Yilmaz, C., 2013. Experimental and numerical evidence for the existence of wide and deep phononic gaps induced by inertial amplification in two-dimensional solid structures, Journal of Sound and Vibration 332, 6389–6404.

[27] Murnaghan, F.D., 1937. Finite deformations of an elastic solid, American Journal of Mathematics 59, 235–260

[28] Pau, A., Lanza di Scalea, F., 2015. Nonlinear guided wave propagation in prestressed plates, The Journal of the Acoustical Society of America 137, 1529–1540.

[29] Dubuc, B., Ebrahimkhanlou, A., Salamone, S., 2017. The effect of applied stress on the phase and group velocity of guided waves in anisotropic plates, The Journal of the Acoustical Society of America 142, 3553–3563.

[30] Mazzotti, M., Marzani, A., Bartoli, I., Viola, E., 2012. Guided waves dispersion analysis for prestressed viscoelastic waveguides by means of the SAFE method, International Journal of Solids and Structures 49, 2359–2372.

[31] Mazzotti, M., Miniaci, M., Bartoli, I., 2017. Band structure analysis of leaky Bloch waves in 2D phononic crystal plates, Ultrasonics 74, 140–143.

[32] Mazzotti, M., Bartoli, I., Miniaci, M., Marzani, A., 2016. Wave dispersion in thin-walled orthotropic waveguides using the first order shear deformation theory, Thin-Walled Structures 103, 128–140.

[33] Collet, M., Ouisse, M., Ruzzene, M., Ichchou, M., 2011. Floquet-Bloch decomposition for the computation of dispersion of two-dimensional periodic, damped mechanical systems, International Journal of Solids and Structures 48, 2837–2848.

[34] Mazzotti, M., Bartoli, I., Marzani, A., 2014. Ultrasonic leaky guided waves in fluid-coupled generic waveguides: hybrid finite-boundary element dispersion analysis and experimental validation, Journal of Applied Physics 115, 143512.